Reprinted from
2012 IEEE MTT-S International conference on Ultra-Wideband (ICUWB), 17. – 20. September 2012 in
Syracuse, New York, USA

Frontend ICs for Impulse Radio Sensing and Communications

H. Schumacher, D. Lin, and A. Trasser

Ulm University, Institute of Electron Devices and Circuits, 89081 Ulm, Germany
Email: hschu@ieee.org

***Abstract*—The chipsets discussed in this paper follow the philosophy that the beauty of impulse radio ultra-wideband lies in its simplicity. They provide fully differential circuit solutions in a low-cost SiGe heterostructure bipolar transistor technology addressing short range radar sensors as well as communication links. At the core, an efficient pulse generator concept allows for spectral tunability as well as biphase modulated pulses. Receiver concepts implement correlation detection for radar and biphase modulation, and energy detection for on-off keying communications and localization. Finally, a successful approach to rapid turn-around transmit/receive modules for monostatic IR UWB radars is presented.**

Keywords: Microwave integrated circuits, Ultra wideband technology, Ultra wideband radar

I. Introduction

Impulse Radio Ultra-wideband (IR-UWB) signalling is a somewhat archaic technique known since the days of Hertz and Marconi, receiving renewed interest when vast tracts of spectrum became available for low spectral power density systems on a non-interference basis. The US Federal Communication Commission (FCC) led this regulatory movement, allocating t3.1-10.6 GHz to UWB systems with spectral power densities below -41.3 dBm/MHz [1]. Europe followed suit and allowed systems to operate, without detect-and-avoid (DAA), between 6-8.5 GHz with equally -41.3 dBm/MHZ EIRP [2]. Other administrations (e.g. Japan, Korea) passed similar rules, alas with sometimes deviating spectral requirements.

IR approaches, by no means the only way to exploit UWB opportunities, present advantages in terms of architectural simplicity. IR-UWB systems have no carrier signal and hence promise low power consumption especially at low signalling rates. Reception can take the form of simple energy detection without synchronization, or correlation reception, especially where syncronization is trivial, such as radar setups with co-located transmitter.

Pulse generation is the core challenge in IR-UWB systems. Approaches include the use of digitally generated m-sequences with added filtering [3], base band generation of envelope waveforms with subsequent up-conversion [4], piecewise approximation of mask-conforming waveforms [5] or direct generation using damped relaxation oscillations [6]. The pulse generator reported here employs a quenched-oscillation concept maintaining the circuit simplicity of the damped relaxation oscillation approach, but introducing tunability of the waveform and avoiding the former's reliance on high Q LC resonators.

Another challenge of IR-UWB systems are extremely broadband low-noise amplifiers. Approaches using complex input matching networks have been reported, but frequently result in high noise figure due to unavoidable losses in the passive network, large chip area, and pulse distortion due to non-constant group velocity. Low-noise amplifiers using resistive negative feedback [7] eliminate the need for on-chip inductors and provide inherently wide bandwidth and low group delay variation. The feedback resistor does add noise, but the penalty is usually lower than that due to complex LC matching networks.

In asymmetrically fed UWB antennas, the groundplane at the lower frequency end is often insufficient, leading to feed line radiation [8] which heavily distorts the radiation pattern. All circuits reported here have a fully differential topology which facilitates packaging and provides a perfect match for symmetrically fed UWB antennas without feedline radiation issues.

II. IC technology

All integrated circuits reported in this work were realized in an inexpensive Si/SiGe HBT technology offered by Telefunken Semiconductors GmbH [9]. Due to a high base doping concentration and resulting low base sheet resistance, the transistors offer maximum frequencies of oscillation up to $\mathrm{f_{max}} = 80\mathrm{GHz}$ despite a minimum feature size of 0.8 μm. Selective collector implants allow two different transistors on the same chip, differing in transit frequency and breakdown voltage: $\mathrm{f_T} = 40\mathrm{GHz}, \mathrm{BV_{CEO}} = 4.5\mathrm{V}$ and $\mathrm{f_T} = 80\mathrm{GHz}, \mathrm{BV_{CEO}} = 2.4\mathrm{V}$, respectively. The technology has proven to be fully adequate for IR UWB applications.

III. Pulse generator design

Figure 1 shows the pulse generator schematic. First, disregard the components with a dashed outline; capacitor $\mathrm{C_{1a}}$ is connected directly in parallel with $\mathrm{L_1}, \mathrm{L_2}$. Transistors $\mathrm{T_5}$ and $\mathrm{T_6}$ form a cross-coupled oscillator, whose resonant frequency, set by $(\mathrm{L_1} + \mathrm{L_2})\mathrm{C_{1a}}$, determines the center frequency of the output spectrum. Its tail transistor $\mathrm{T_2}$ forms half of a current mirror, starting to conduct if the collector potential of $\mathrm{T_4}$ is sufficiently high. $\mathrm{T_3}$ and $\mathrm{T_4}$ form a Schmitt trigger, creating a fast rising edge at the collector of $\mathrm{T_4}$. After an initial sharp

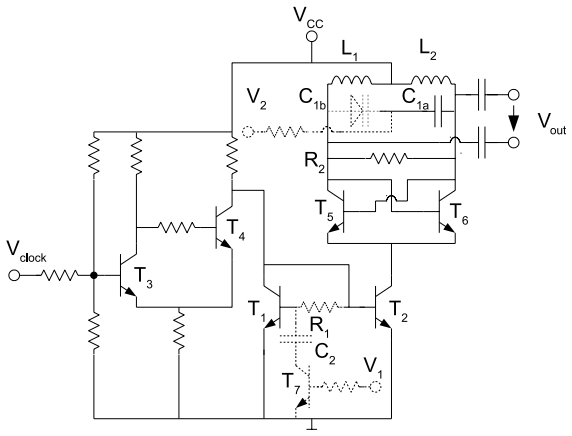

Fig. 1. Circuit schematic of the UWB pulse generator. The dashed component outlines show the extension for tunability of the pulse shape for different spectral masks.

increase, the collector potential of T_4 is pulled down again to a lower constant value by the current mirror. T_2 will conduct only briefly during the initial voltage surge at the collector of T_4, creating the envelope of the output pulse, determined predominantly by the time constant $\mathrm{R}_1\mathrm{C}_{\mathrm{be,T1}}$.

The two parameters which determine the pulse parameters (oscillation frequency and envelope) are easily modified. This is shown by the dashed components in Fig. 1. The tank circuit capacitance is now formed by $\mathrm{C}_{1\mathrm{a}}$ in series with the varactor $\mathrm{C}_{1\mathrm{b}}$. The envelope is modified by changing the capacitance between the base of T_1 and ground, via C_2 and T_7, switching C_2 in and out.

Depending on voltages V_1 and V_2, the emitted pulses conform to the FCC ($\mathrm{V}_1 = 0\mathrm{V}, \mathrm{V}_2 = 2\mathrm{V}$), ECC ($\mathrm{V}_1 = 1\mathrm{V}, \mathrm{V}_2 = 2.3\mathrm{V}$), or Japanese masks ($\mathrm{V}_1 = 1\mathrm{V}, \mathrm{V}_2 = 6\mathrm{V}$) [10]. At 100 MHz pulse repetition frequency, the DC power consumption is 6 mW for the FCC setting, and 10 mW for the other settings. Fig. 2 shows, as an example, the pulse form and spectral compliance when set to the ECC mask.

A. Pulse generator with biphase modulation capability

In the pulse generator design, a slight asymmetry in the cross-coupled pair ($\mathrm{T}_5, \mathrm{T}_6$ in Fig. 1) ensures that the oscillation always starts with the same phase. Biphase modulation capability can be introduced by modifying the currents flowing in the individual branches. Consider Fig. 3. Additional branch currents are set through current mirrors $\mathrm{T}_7, \mathrm{T}_9$ and $\mathrm{T}_8, \mathrm{T}_{10}$. If DATA is low, T_7 blocks and T_8 conducts. If DATA is high, T_7 conducts, T_{11} switches into saturation and T_8 blocks. Thus, oscillation will start in one of two phase states once T_2 is turned on, constituting biphase modulation, as shown in Fig. 4.

IV. Receiver design

The next section will describe two different types of receivers for IR-UWB. Energy detection receivers for on-off keying (OOK) and localization applications do not need synchronization with a remote transmitter. They are conceptively

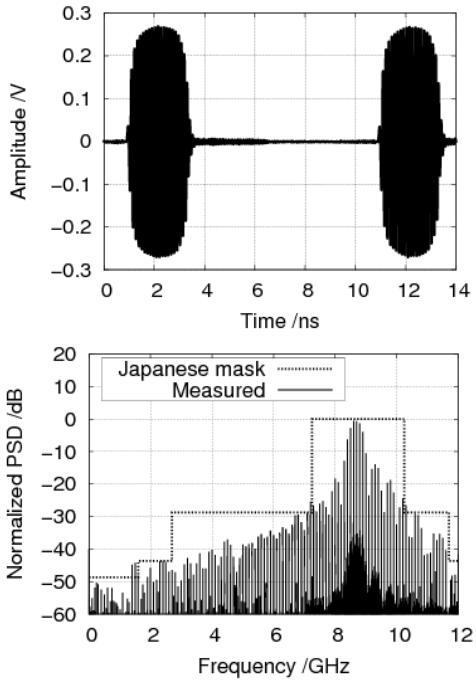

Fig. 2. Time domain waveform (top) and spectrum (bottom) of the tunable pulse generator output signal set for compliance with the ECC UWB mask.

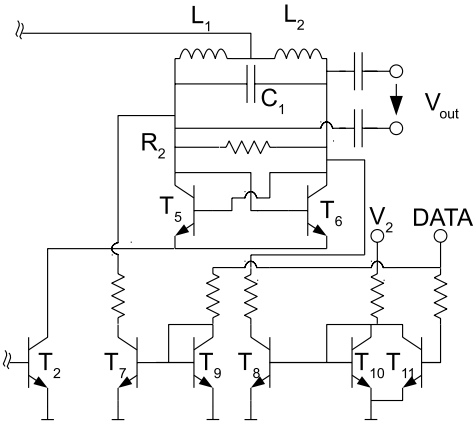

Fig. 3. Adding biphase capability to the pulse generator in Fig. 1.

very simple, but sensitive to interference. Correlation-type receivers compare the received pulse form with a delayed replica. They are more robust to interference, but require exact synchronization with the transmitter. In a radar setup, this is easy to accomplish as will be shown.

Key components of both receiver types are

- a low noise amplifier with sufficient bandwidth, low group velocity variation, and low noise figure across the full band,
- a four quadrant analog multiplier performing the squaring operation in the energy detection receiver, and the multiplication with the template pulse in the correlation receiver, and
- a low-pass filter performing envelope detection in the en-

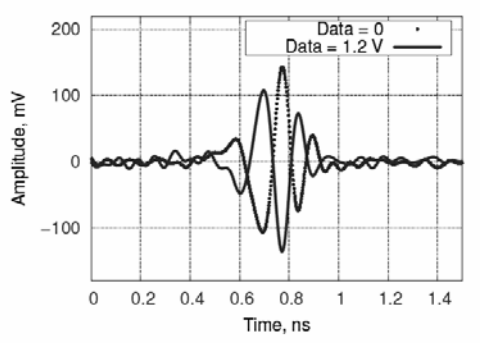

Fig. 4. Biphase modulated output signal of the pulse generator shown in Fig. 3.

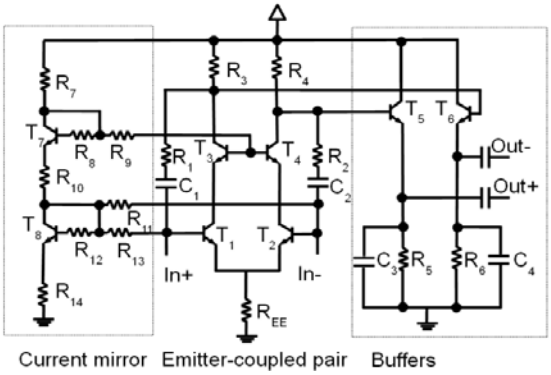

Fig. 5. Schematic diagram of the fully differential UWB low-noise amplifier.

ergy detection, and integration in the correlation receiver. To allow flexible use of the receiver ICs, the on-chip low-pass filter has a high cut-off frequency at 900 MHz, and is usually followed by a much narrower off-chip low-pass filter, especially in case of vital sign detection.

A. UWB low noise amplifier

Fig. 5 depicts the fully differential low-noise amplifier schematic. T_1 through T_4 form a differential cascode biased by the stacked current mirror $\mathrm{T}_7, \mathrm{T}_8$. Input match and broadband voltage gain is achieved simultaneously by transistor scaling and resistive negative feedback (resistors $\mathrm{R}_1, \mathrm{R}_2$). $\mathrm{T}_5, \mathrm{T}_6$ form a differential emitter follower buffer.

The design is completely inductor-less, with a chip size of only $(0.38 \cdot 0.37)\ \mathrm{mm}^2$, including bond pads. The LNA provides 20 dB gain from 1-12 GHz, and a group delay variation $\Delta\tau_{\mathrm{gd}} = 15\mathrm{ps}_{\mathrm{P-P}}$ over the full FCC UWB band. The differential noise figure varies between 2 dB at 3 GHz and 2.9 dB at 10.6 GHz. The power consumption is 77 mW.

B. Energy detection receiver

The core of the energy detection receiver is a Gilbert cell four quadrant multiplier. Fig. 6 shows that the signal fed to the lower differential pair of the Gilbert cell is taken directly from the LNA output transistors, while the signal fed to the top quad is passed first through the emitter follower buffer. The time delay in both paths is equal, ensuring proper squaring

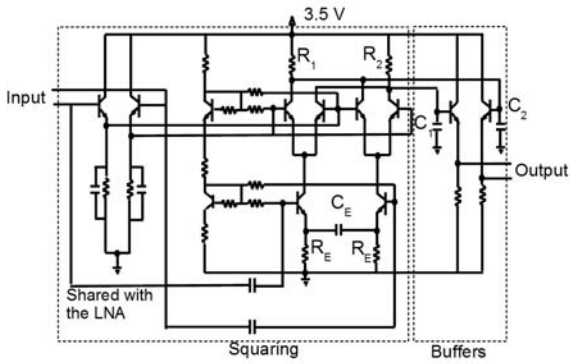

Fig. 6. Squaring and low-pass filter circuit of the energy detection receiver. The LNA from Fig. 5 is added to complete the IC.

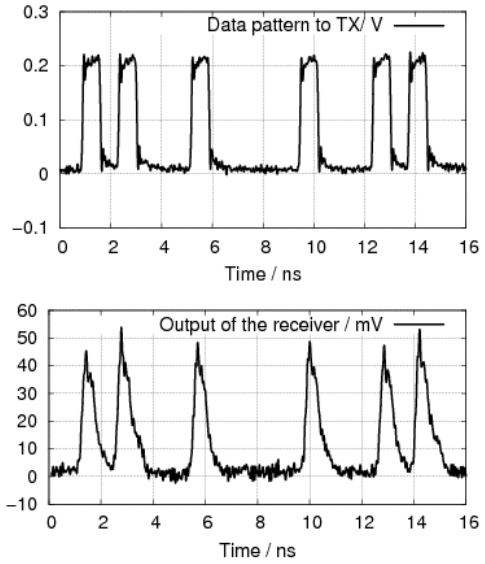

Fig. 7. On-off keying transmission experiment at 700 Mbit/s over 25 cm, using the pulse generator in Fig. 1 and the energy detection receiver IC. Top trace: signals at the pulse generator input, bottom trace: detected signal at the receiver output.

operation. The capacitors C_1 and C_2 provide the low-pass function needed for the envelope detection. The complete receiver IC measures $(0.43{\cdot}0.61)\mathrm{mm}^2$ and consumes 108 mW.

To test the energy detection receiver, a 700 Mbit/s RZ pulse train was generated with the pulse generator described above (Fig. 1), consuming 7.5 mW here. Transmitter and receiver were connected to dipole-fed circular slot antennas [11], placed at 25 cm distance. Fig. 7 shows the input pulse sequence from a bit pattern generator (top) and the corresponding detected pulse envelopes at the output of the receiver IC, with a peak amplitude of 50 mV for the pulses. This experiment clearly shows the capability of the simple transmitter/receiver combination to transmit significant bitrates over short distances.

C. Monolithic correlation receiver

The template signal of the correlation receiver is generated on chip by a dedicated pulse generator, avoiding the need

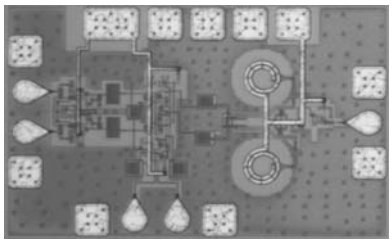

Fig. 8. Chip micrograph of the differential fully monolithic correlation receiver.

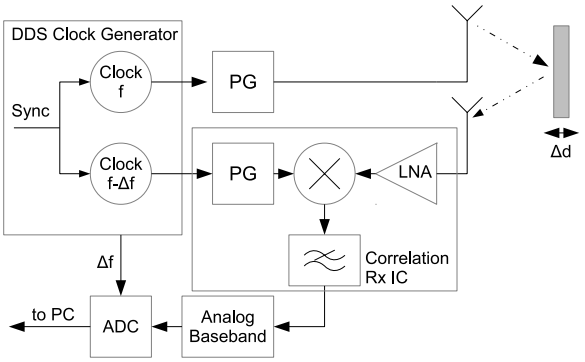

Fig. 9. Block diagram of the UWB radar system used for vital sign detection.

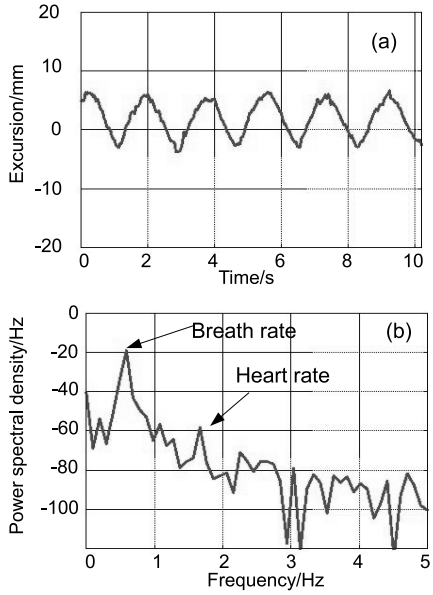

Fig. 10. Time domain (a) and spectral domain (b) measurement of vital signs using IR-UWB radar on a test person with pronounced tachypnea.

to provide an adjustable ultra-wideband true time delay. The transmit and receive clocks in the radar setup need to be phase adjusted only, which is simple and in practice done using a DDS board, as shown in Fig. 9.

The low-noise amplifier is identical to the one described above, the multiplier is realized using a Gilbert cell operated in the analog regime, and the low-pass filter is implemented in the buffer as shown for the case of the energy detection receiver above.

The IC, shown in Fig. 8, measures $(0.57 \cdot 0.89)\ \mathrm{mm}^2$ and consumes a total DC power of 130 mW. This is a reduction by a factor of three compared to the single-ended monolithic correlation receiver published earlier [12].

V. UWB RADAR FRONTENDS

A common application for IR-UWB radar systems is detection of vital signs. Here, the UWB pulse is reflected off the patient's thorax or abdominal region, and correlation detection is used to track minute movements of the target region. In our experiments, mechanical movements below 1 mm amplitude can be cleanly detected. The measurement principle is shown in Fig. 9.

The setup is controlled by a DDS clock generator, which outputs two clock signals with a small (100 Hz) frequency offset $\Delta\mathrm{f}$, as well as the frequency difference $\Delta\mathrm{f}$ itself. The two clocks are fed to the transmit pulse generator and the template pulse generator on the correlation receiver IC, respectively. This generates a periodically varying time delay between receiver and transmitter, which results in a sweeping cross-correlation measurement. The output of the receiver IC is further lowpass filtered in an analog baseband circuit ($\mathrm{f_c} = 25\mathrm{kHz}$) and fed to a dual-channel analog/digital converter (ADC). The frequency offset $\Delta\mathrm{f}$ is fed to the other channel. The PC program then tracks the peak amplitude of the cross correlation as a function of the time-varying delay, which can be calibrated to distance.

The strong crosstalk component due to crosstalk between receive and transmit antennas is easily identified and removed by time gating, a significant advantage of this technique over e.g. m-sequence UWB systems. Figure 10 shows a sample measurement for an adult male with pronounced tachypnea (respiratory rate approx. 32/min) seated 24 cm away from the sensor. This measurement was performed with an earlier, single-ended frontend connected to Vivaldi antennas for transmit and receive, but very similar results are expected for the newer differential frontend.

The time domain data is Fourier transformed to the spectral domain, where the spectral component of the breath rate is clearly resolved. The heart rate component is also visible, but robust extraction needs further signal processing which is not undertaken here. The heart rate detection is due to vibrations of the chest wall, not due to movement of the heart muscle itself.

All IR-UWB systems so far, including the one described above, use separate receive and transmit antennas. Monostatic radar frontends would lead to a significant reduction in the overall size of IR-UWB sensors due to the elimination of one antenna, however the problem is generally the rapid (nanosecond) switching between transmit and receive paths. The authors are currently exploring a different monostatic frontend concept, shown in Fig. 11, which does not employ a transmit/receive switch. Here, a buffer amplifier following the pulse generator and the low-noise amplifier are tied together at the input and connected to a single antenna. The added

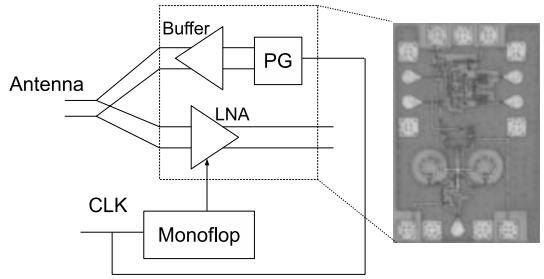

Fig. 11. Block diagram and chip photo of the experimental monostatic radar frontend.

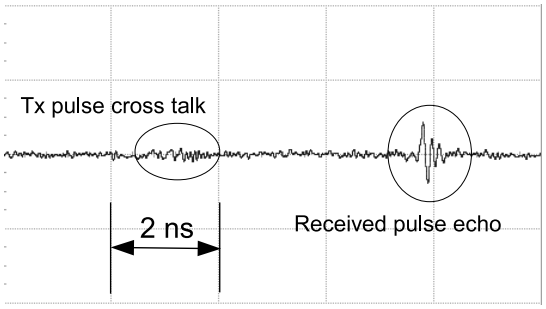

Fig. 12. Real time oscilloscope trace showing the functional test of the monostatic radar frontend, displaying transmitted pulse crosstalk and received pulse echo.

parasitics of the opposing circuit block are included in the design of buffer amplifier and LNA, respectively. During emission of the pulse, the LNA bias is temporarily removed using an (external) monoflop and a bandgap reference circuit. After the pulse has been transmitted, the LNA bias is restored, and the amplifier returns to full gain and sensitivity within 1.5 ns.

In a first functional test, the antenna terminal is connected to two short coaxial cables, each fed into a 10 dB attenuator shorted at the far end. Cable and attenuator result in a delay of 2.5 ns, or 75 cm in air to the target. Fig. 12 shows the resulting time domain trace on a real time oscilloscope, displaying the differential output voltage of the LNA. Due to the high isolation of the 'cold' low-noise amplifier, the crosstalk from the transmitted pulse is barely visible and much lower than for the bistatic arrangement. The received echo is cleanly resolved. In a next step, this circuit will be included in a full UWB short-range radar arrangement.

It should be noted that the bias switching results in significant common-mode transients at the LNA output. Due to the carefully balanced differential setup, these transients are completely invisible in the differential output signal displayed here.

With the successful demonstration of the monostatic frontend, IR-UWB radars can be further simplified, with only a single antenna and a single transmit/receive module at the antenna feed point.

VI. Conclusions

Using an inexpensive Si/SiGe HBT technology, a flexible, fully differential chipset for impulse radio ultra-wideband applications was presented. A pulse generator using a Schmitt trigger for clock shaping and a quenched cross-coupled oscillator features low power consumption and highly stable pulse generation. It can be easily extended to include tunability to various UWB spectral masks as well as biphase modulation capability. Building upon a low-noise amplifier with negative feedback, 20 dB gain, 15 ps group delay variation and 2.9 dB worst-case noise figure across the FCC UWB band, receivers using energy detection for simple on-off keying communications as well as localization applications, and a fully monolithic correlation receiver for short range UWB radar applications were realized. Application of an IR-UWB radar system for vital sign detection was demonstrated. Finally, a rapid turn-around transmit/receive module IC for a monostatic UWB radar frontend was demonstrated for the very first time, with negligible crosstalk from the transmitted pulse.

Acknowledgment

The authors gratefully acknowledge the financial assistance of the German Research Foundation DFG for this work, and the continued cooperation of Telefunken Semiconductors GmbH in the fabrication of the ICs.

References

[1] FCC, "Revision of Part 15 of the Commission's Rules Regarding Ultra-Wideband Transmission Systems"; Report and Order, ET Docket No. 98–153, released 15 July 2002.

[2] ECC decision ECC/DEC/(6)12.

[3] J. Sachs, R. Herrmann, M. Kmec, M. Helbig and K. Schilling, "Recent Advances and Applications of M-Sequence based Ultra-Wideband Sensors"; *IEEE International Conference on Ultra-Wideband (ICUWB)*, Singapore, 24-26 Sept. 2007, pp. 50–55.

[4] Y. Zheng et al., "A 0.18μm CMOS Dual-Band UWB Transceiver"; *ISSCC Dig. Tech. Papers,* San Francisco, CA, 11-15 Feb. 2007, pp. 114–115.

[5] X. Wang et al., "A Whole-Chip ESD-Protected 0.14-pJ/p-mV 3.1-10.6 GHz Impulse-Radio UWB Transmitter in 0.18μm CMOS"; *IEEE Transactions on Microwave Theory and Techniques*, Vol. 59, no. 4, pp.1109–1116, 2011.

[6] J. Dederer, B. Schleicher, F. De Andrade Tabarani Santos, A. Trasser and H. Schumacher, "FCC compliant 3.1-10.6 GHz UWB Pulse Radar using Correlation Detection"; *Proc. IEEE MTT-S Int. Microw. Symp.*, Honolulu, HI, 3-8 June 2007, pp. 1471–1474.

[7] J. Dederer, S. Chartier, T. Feger, U. Spitzberg, A. Trasser, and H.Schumacher, "Highly Compact 3.1-10.6 GHz UWB LNA in SiGe HBT Technology"; Proc. Europ. Microwave Integrated Circuits Conf., Munich, Germany, 8–10 Oct. 2007, pp. 247-250.

[8] T.W. Hertel, "Cable-current effects of miniature UWB antennas"; IEEE Int. Antenna and Prop. Symp., Vol. 3A, pp. 524–527, 2005.

[9] Telefunken Semiconductors SiGe2RF, see http://www.telefunkensemi.com/foundry/rf-technology.html (accessed 23 Feb 2012).

[10] D. Lin, B. Schleicher, A. Trasser, and H. Schumacher, "Si/SiGe HBT UWB impulse generator tunable to FCC, ECC and Japanese spectral masks"; IEEE Radio and Wireless Symp., Phoenix, AZ, 16-19 Jan. 2011, pp. 66–69.

[11] M. Leib, M. Frei, W. Menzel, "A novel ultra-wideband circular slot antenna excited with a dipole element"; *IEEE International Conference on Ultra-Wideband (ICUWB)*, 9-11 Sept. 2009, pp. 386–390.

[12] J. Dederer, B. Schleicher, A. Trasser, T. Feger and H. Schumacher, "A fully monolithic 3.1-10.6 GHz UWB Si/SiGe HBT Impulse-UWB correlation receiver"; *IEEE International Conference on Ultra-Wideband (ICUWB)*, Hannover, Germany, 10-12 Sep. 2008, pp. 33–36.